Original article

Synthesis, *in vitro* binding studies and docking of long-chain arylpiperazine nitroquipazine analogues, as potential serotonin transporter inhibitors

Małgorzata Jarończyk [a,*], Karol Wołosewicz [b], Mari Gabrielsen [c], Gabriel Nowak [d], Irina Kufareva [e], Aleksander P. Mazurek [a,f], Aina W. Ravna [c], Ruben Abagyan [e], Andrzej J. Bojarski [d], Ingebrigt Sylte [c], Zdzisław Chilmonczyk [a]

[a] National Medicines Institute, 30/34 Chełmska Street, 00-725 Warsaw, Poland
[b] Institute of Chemistry, University of Bialystok, Al. Pilsudskiego 11/4, 15-443 Bialystok, Poland
[c] Medical Pharmacology and Toxicology, Department of Medical Biology, Faculty of Health Science, University of Tromsø, N-9037 Tromsø, Norway
[d] Institute of Pharmacology PAS, Smętna Street 12, 31-343 Cracow, Poland
[e] Skaggs School of Pharmacy and Pharmaceutical Sciences, 9500 Gilman Drive, MC 0747 La Jolla, California 92093-0747, USA
[f] Medical University of Warsaw, Faculty of Pharmacy, 1 Banacha Street, 02-097 Warsaw, Poland

ARTICLE INFO

ABSTRACT

It is well known that 6-nitroquipazine exhibits about 150-fold higher affinity for the serotonin transporter (SERT) than quipazine and recently we showed quipazine buspirone analogues with high to moderate SERT affinity. Now we have designed and synthesized several 6-nitroquipazine buspirone derivatives. Unexpectedly, their SERT binding affinities were moderate, and much lower than that of the previously studied quipazine buspirone analogues. To explain these findings, docking studies of both groups of compounds into two different homology models of human SERT was performed using a flexible target-ligand docking approach (4D docking). The crystal structures of leucine transporter from *Aquifex aeolicus* in complex with leucine and with tryptophan were used as templates for the SERT models in closed and outward-facing conformations, respectively. We found that the latter conformation represents the most reliable model for binding of buspirone analogues. Docking into that model showed that the nitrated compounds acquire a rod like shape in the binding pocket with polar groups (nitro- and imido-) at the ends of the rod. 6-Nitro substituents gave steric clashes with amino acids located at the extracellular loop 4, which may explain their lower affinity than corresponding quipazine buspirone analogues. The results from the present study may suggest chemical design strategies to improve the SERT modulators.

© 2012 Elsevier Masson SAS. All rights reserved.

1. Introduction

The serotonin transporter (SERT), together with the dopamine and noradrenaline transporters, belongs to the neurotransmitter:sodium symporter family (NSS) [1]. SERT acts as a co-transporter of sodium and chloride ions, and serotonin molecules [2–4]. The human SERT consists of 630 amino acids with 12 transmembrane domains and cytoplasmic N- and C-terminals [5,6]. According to site directed mutagenesis Tyr^{95} and Asp^{98}, located in the first transmembrane helix (TMH), are crucial for serotonin binding [7,8].

SERT is the target for several antidepressant drugs including the selective serotonin reuptake inhibitors (SSRIs) [9]. SSRIs are today the most widely used agents for the treatment of depression and many other related disorders [10,11]. The SSRIs act by blocking serotonin reuptake thus increasing the concentration of serotonin at the synapse, enhancing the serotonergic neuronal transmission. A variety of SSRIs such as fluoxetine and paroxetine have been developed for the treatment of depression [14,15]. However, because a large number of neurological and psychiatric diseases are associated with transporter defects it is a considerable interest in identification of novel and improved SERT modulators. The disadvantages of the available SSRIs include multiple side-effects, such as anxiety, impotency, and sleep disorders, as well as a delayed onset of action: it may take about 6–8 weeks for the effects of the drugs to develop [12,13]. Thus, safer and more effective therapeutic agents are needed.

In our former papers we described synthesis and biological evaluation of a series of quipazine buspirone analogues with moderate affinity for SERT (Table 1, compounds **12–19**) [16–20]. 6-Nitroquipazine (**1**, Table 1) is known as one of the most potent and

selective inhibitors of SERT *in vitro* [21,22] and *in vivo* [23,24]. Its nitro group plays an important role in retaining sub-nanomolar affinity to SERT (K_i = 0.17 nM) [26], since removing the group diminishes the affinity substantially (quipazine K_i = 30 nM [25]). Since 6-nitroquipazine (**1**) exhibits approximately 150 times higher affinity to SERT than quipazine (**2**) we decided to prepare and evaluate the affinity of several buspirone-like 6-nitroquipazine derivatives with similar substituents as our previous quipazine buspirone analogues (Table 1). Several papers describe structure−affinity relationship for aromatic and piperazine ring substituted 6-nitroquipazines [27−29] but only two describing single N-4 substituted 6-nitroquipazine derivatives [30,31].

Molecular modelling studies of ligand interactions with SERT were performed in order to investigate the structural differences in SERT binding between the compounds.

The leucine transporter (LeuT) is a bacterial homologue of SERT which belongs to Na$^+$/Cl$^-$ -dependent transporter family [32]. In our previous paper [33] a SERT model was built using the X-ray crystal structure of the leucine transporter (LeuT) from *Aquifex aeolicus* [32] in complex with leucine as template for the homology modelling. This LeuT structure is believed to represent the substrate occluded conformation, and was interpreted as a conformational intermediate between inward and outward-facing conformations. In 2008, the structure of LeuT in complex with tryptophan in an outward-facing (open-to-out) conformation was published [34]. The recently developed homology model of SERT in the open-to-out conformation [37] was used in the present study. The compounds (Table 1) were docked to both SERT models and analyzed using molecular modelling methods. The predicted models were analyzed for their ability to explain the weak binding of the synthesized 6-nitroquipazine buspirone analogues and suggest different chemical strategies for improvement of SERT modulators.

2. Materials and methods

2.1. Synthesis

The synthesis of compounds **12−19** was described previously [16−19]. The synthesis of compounds **3−11** was as follows:

Table 1
The molecular structure and affinities to SERT (IC$_{50}$, nM) and 5-HT$_{1A}$ receptor affinities (K_i, nM) of the studied compounds. In the brackets the inhibition constant of [^{3}H]5-HT at human tissue is included.

Compound	R^1	R^2	R^3	n	R^4	SERT IC$_{50}$ ± SEM, nM	5-HT$_{1A}$ K_i ± SEM, nM
1	NO$_2$	H	H	−	H	ND (K_i = 0.17 nM)	ND
2	H	H	H	−	H	ND (K_i = 30 nM)	230
3	NO$_2$	CH$_3$	H	4	b	267.8 ± 26.3	711.0 ± 21.0
4	NO$_2$	H	H	4	b	921.1 ± 8.2	10600 ± 3500
5	NO$_2$	CH$_3$	H	4	c	1350 ± 211	776.5 ± 117.5
6	NO$_2$	H	H	4	c	25900 ± 1100	1100 ± 400
7	NO$_2$	CH$_3$	H	4	d	806.8 ± 85.2	221.0 ± 34.6
8	NO$_2$	H	H	4	d	616.3 ± 1.1	2100 ± 400
9	NO$_2$	H	H	4	a	4130 ± 900	59000 ± 23100
10	H	H	Cl	4	d	2800 ± 200	1400 ± 100
11	C(O)NHCH$_3$	H	H	4	c	18800 ± 700	3200 ± 800
12	H	CH$_3$	H	4	a	33.4 ± 17.0 (8)[a]	13[17]
13	H	H	H	4	a	95.5 ± 37.2	39[17]
14	H	CH$_3$	H	3	a	(80)[a]	275[19]
15	H	CH$_3$	H	4	b	(50)[a]	37 ± 6[18]
16	H	CH$_3$	H	4	c	75.0 ± 16.3	24 ± 3[18]
17	H	H	H	4	c	111.6 ± 27.2	39 ± 7[16]
18	H	CH$_3$	H	4	d	170.7 ± 68.5	15 ± 3[18]
19	H	H	H	4	d	146.4 ± 19.4	11 ± 2[16]

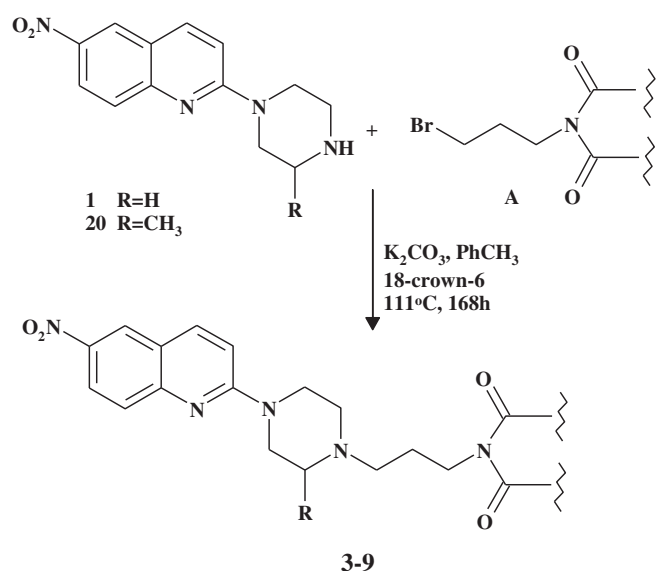[a] data obtained from Servier laboratories.

Fig. 1. General scheme of the preparation of 6-nitroquipazine buspirone analogues **3–9**.

2.1.1. Compounds **3−9**

Compounds **3−9** were prepared by the condensation of 6-nitroquipazine (**1**) or 3′-methyl-6-nitroquipazine (**20**) with bromobutylimide (**A**) (Fig. 1), whereas starting (**1**) and (**20**) were prepared as described in [26,27], respectively.

Fragments of the general structure **A** were synthesized by the condensation of imides (**21−24**) with 1,4-dibromobutane to give bromobutyloimides (**25−28**) (Fig. 2).
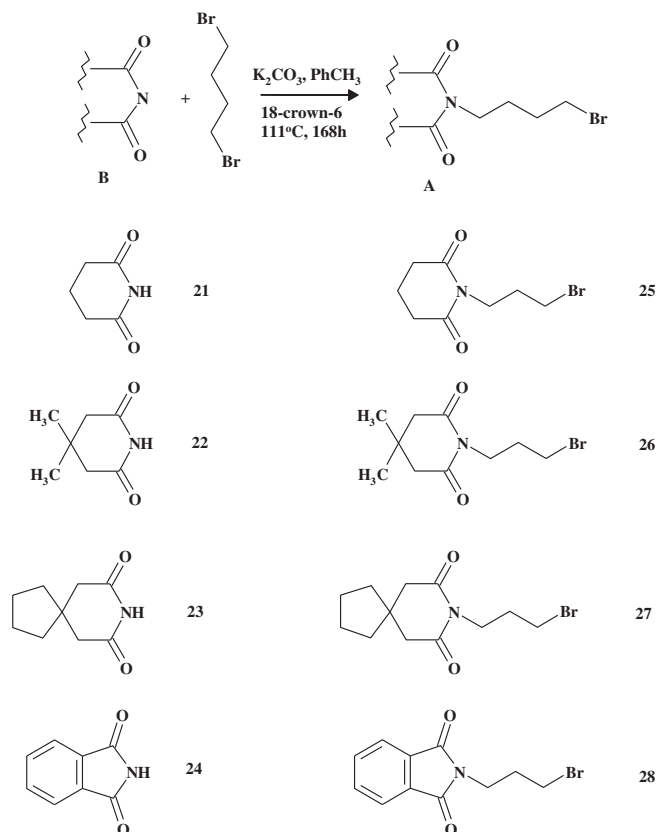

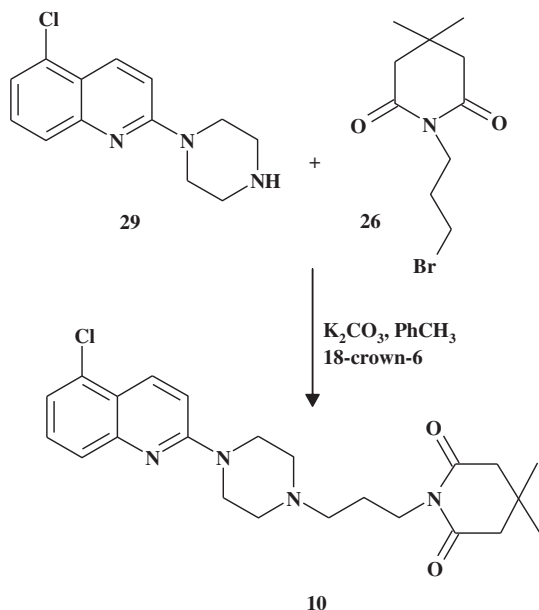**Fig. 2.** Synthesis of bromobutylimides (A) **17−20**.

Fig. 3. Synthesis of 5-chloro derivative **10**.
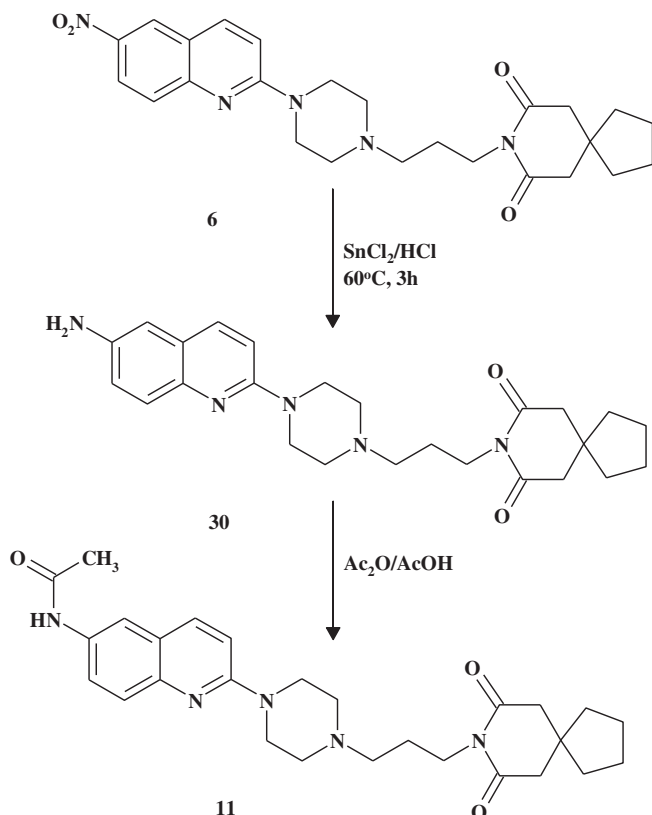
2.2. SERT binding experiments

The assay was performed according to the method of Owens et al. [35] with slight modifications. Rat cerebral cortex was homogenized in 30 volumes of ice-cold 50 mM Tris−HCl containing 150 mM NaCl and 5 mM KCl, pH = 7.7 at 25° C and centrifuged at $20,000 \times g$ for 20 min. The supernatant was decanted and the pellet was resuspended in 30 volumes of buffer and centrifuged again. The resulting pellet was resuspended in the same quantity of the buffer and centrifuged for the third time in the same conditions. [^{3}H]-Citalopram (spec. act. 50 Ci/mmol, NEN Chemicals) was used for labelling 5-HT-transporter. 240 μl of the tissue suspension, 30 μl of 1 μM imipramine (displacer), 30 μl of 1 nM [^{3}H]-Citalopram and 100 μl of the analyzed compound were incubated at 22 °C for 1 h. The concentrations of the analyzed compounds ranged from 10^{-10} to 10^{-4} M.

Incubations were terminated by vacuum filtration over Whatman GF/B filters and washed two times with 100 μl of ice-cold buffer. Radioactivity was measured in a WALLAC 1409 DSA − liquid scintillation counter. All assays were done in duplicates.

2.3. 5-HT$_{1A}$ receptor binding experiments

[^{3}H]-8-Hydroxy-2-(di-n-propylamino)-tetralin ([^{3}H]-8−OH−DPAT, spec. act. 106 Ci/mmol, NEN Chemicals) was used for labelling 5-HT$_{1A}$ receptors. The membrane preparation and the assay procedure were carried out according to the published procedure [36] with slight modifications. Briefly, the cerebral cortex tissue was homogenized in 20 vol. of 50 mM Tris−HCl buffer (pH 7.7 at 25 °C) using Ultra-Turrax® T 25, and was then centrifuged at 32000 g for 10 min. The supernatant fraction was discarded, and pellet was resuspended in the same volume of Tris−HCl buffer and was then centrifuged. Before the third centrifugation, the samples were incubated at 37 °C for 10 min. The final pellet was resuspended in Tris−HCl buffer containing 10 μM pargyline, 4 mM CaCl$_2$ and 0.1% ascorbic acid. One millilitre of the tissue suspension (9 mg of wet weight), 100 μl of 10 μM serotonin (for unspecific binding), 100 μl of [^{3}H]-8−OH−DPAT and 100 μl of analyzed compound were incubated at 37 °C for 15 min. The incubation was followed by a rapid vacuum filtration through Whatman GF/B glass filters, and was when washed 3 times with 5 mL of a cold buffer (50 mM Tris−HCl, pH 7.7) using a Brandel cell harvester. The final [^{3}H]-8−OH−DPAT concentration was 1 nM, and the concentrations of the analyzed compounds ranged from 10^{-10} to 10^{-4} M.

2.1.2. Compounds 10 and 11

The 5-Chloroquipazine derivative (**10**) was prepared by the condensation of 5-chloroquipazine (**29**) with imide **26** (Fig. 3), while 6-acetamido derivative (**11**) was obtained from the nitro derivative **6** by reduction with tin/hydrochloric acid followed by acetylation (Fig. 4).

2.4. Molecular modelling

2.4.1. SERT models

Two SERT models representing different conformational states were used in the present study. The templates for homology modelling of SERT were crystal structures of the leucine transporter from A. aeolicus: (i) in complex with leucine (PDB-id: 2A65) [32] and (ii) in complex with tryptophan (PDB-id: 3F3A) [34]. The first SERT model, closed at both sites of the membrane, represents a substrate-bound (occluded) conformation (Fig. 5a), whereas the second, corresponds to the open-to-out conformation (Fig. 5b).

The generation of SERT homology models has been described in detail in two other papers (occluded [33], open-to-out [37]). A comprehensive alignment of NSS family members from the literature [40] was used to guide the alignment of the SERT (UniProt [38] accession number P31645) and LeuT sequences. The homology models were generated using the BuildModel macro available in ICM (Internal Coordinate Mechanics) [39]. Energy refinement of SERT models was performed using the RefineModel macro of ICM, which gradually relaxes the model using the
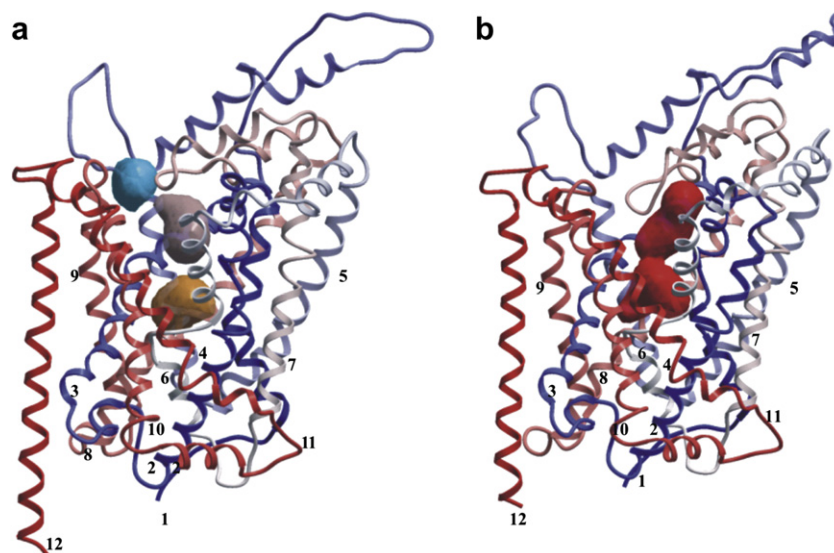

Fig. 4. Synthesis of 6-amido derivative **11**.

Fig. 5. Serotonin transporter (SERT) models based on the X-ray structure of the LeuT$_{Aa}$ from *Aquifex aeolicus*: (a) The substrate occluded conformation, (b) The outward-facing conformation. The models are coloured from amino (red) to carboxy (blue) terminal. Binding pockets identified by using ICM PocketFinder: putative binding pocket is displayed in orange colour, vestibular binding pocket, consisting of the two subpockets, is displayed in a blue and pink colour. The large binding pocket of SERT in the outward-facing conformation is displayed in red colour. (For interpretation of the references to colour in this figure legend, the reader is referred to the web version of this article.)

combination of the ICM force field [41] and harmonic positional restraints with the strength adjusted to counter the initial conformational stress. The RefineModel refinement was followed by regularisation, i.e., fitting the amino acids with the ideal covalent geometry. The loops were included in both SERT models and were present during docking.

2.4.2. Docking

The ligands were docked both using a regular rigid receptor-flexible ligand docking approach [39] and a new ensemble docking approach (described in detail in another paper [37]). SERT conformational ensembles were prepared in two steps: (i) detection of a ligand binding pocket using ICM PocketFinder (tolerance level 3) [65], and (ii) generation of different SERT binding pocket conformations by biased probability Monte Carlo (BPMC [41]) sampling of the binding site amino acid side chains in the presence of repulsive grid density representing a generic ligand. Each ligand was docked simultaneously into all SERT conformations using the four-dimensional (4D) flexible ligand docking [42]. During the 4D docking, the receptor conformations represent the fourth dimension [42]. The 3D grids of each conformation are stored as a single data structure, and serve as a variable in the global optimization. This allows ligand docking to the multiple binding pocket conformations in a single docking simulation.

Prior to docking the ligand sampling in vacuo was performed. A set of ligands conformers generated was placed into the binding site in four principal orientations and used as starting points for Monte Carlo global energy optimization.

The binding scores of the docked compounds were predicted using the VLS scoring function implemented in ICM [43,44]. The VLS scoring function consists of the internal force field energy of the ligand and the ligand-receptor interaction energy. The ligand-receptor interaction energy includes several weighted terms: van der Waals, a hydrophobicity term based on the solvent accessible surface buried upon binding, an electrostatic solvation term calculated using a boundary-element solution of the Poisson equation, hydrogen−bond interactions and an entropic term proportional to the number of flexible torsions in the ligand.

2.4.3. Detection of binding pockets, side chain sampling and docking

Three putative binding pockets were identified in the occluded SERT model: one pocket in an area corresponding to the binding pocket of the substrate leucine in the LeuT structure [32] that is believed to represent the substrate binding pocket of SERT, and two pockets in the vestibular region of the model (Fig. 5a). Superimposition of the SERT homology model with the LeuT crystal structures cocrystallised with SERT inhibitors (PDB-id: 3GWW, 3GWV, 3GWU, 2Q6H, 2Q72, 2QB4, 2QEI and 2QJU) showed that the ligands were located in an area of LeuT corresponding to the two vestibular binding pockets of the SERT model. Thus, based on the similarities with LeuT a binding pocket in SERT may consist of amino acids located in the two vestibular binding pockets of SERT. Further, the superimposition also revealed that parts of the cocrystallised inhibitors were in a region corresponding to the region occupied by the amino acids at the tip of EL4 of our SERT model.

The two vestibular binding pockets were separated by parts of an insert into EL4 only, and thus are located in a structurally uncertain region of the model. In order to check if the buspirone analogues could bind SERT in pocket similar to TCA/SSRI in LeuT we decided to fuse these pockets into one and then see of the present compounds could bind. In order to generate one fused vestibular binding pocket to be used as input for BPMC side chain sampling [41], two identical occluded SERT homology models were superimposed, and the tip of EL4 (amino acids 398−402) was removed from one of the models. ICM PocketFinder [65] was then used to identify a fused binding pocket in the altered model (lacking the tip of EL4) before the model was removed, while the pocket was kept. The unchanged model with the fused binding pocket (generated from the other model lacking the EL4 tip) was used as an input for the conformational ensemble generation routine. During second step of the protocol, the side chains of amino acids Leu^{99}, Trp^{103}, Arg^{104}, Tyr^{107}, Tyr^{175}, Tyr^{176}, Ile^{179}, Trp^{182}, Tyr^{232}, Val^{236}, Gln^{238}, Ile^{251}, Asp^{328}, Phe^{335}, Lys^{399}, Asp^{400}, Ser^{404}, Leu^{406}, Ile^{408}, Leu^{481}, Tyr^{487}, Val^{489}, Lys^{490}, Glu^{494}, Arg^{564} and Tyr^{568} were sampled using BPMC [41] in the presence of a repulsive grid density representing a generic ligand. Out of 45 generated binding pocket

conformations, five were selected and used for 4D docking to the fused vestibular binding pocket.

Similarly, five conformations of the putative substrate binding site were generated. The following side chains were sampled using BPMC [41]: Tyr[95], Asp[98], Ile[172], Tyr[176], Phe[335], Ser[336], Phe[341], Val[343] and Ser[438].

In the previous study [37] the studied compounds bound mainly to 5 conformations of the SERT model, and thus, these conformations were used for docking in the present study.

In the model of SERT in an open-to-out conformation, one larger binding pocket was detected consisting of amino acids in both the putative substrate binding pocket, and two vestibular pockets of the substrate occluded conformation (Fig. 5b). The side chains of amino acids Tyr[95], Asp[98], Leu[99], Trp[103], Arg[104], Tyr[107], Tyr[175], Tyr[176], Ile[179], Phe[335], Ser[336], Leu[337], Phe[341], Val[343], Lys[399], Asp[400], Pro[403], Leu[405], Leu[406], Phe[407], Ser[438], Thr[439], Glu[493] and Thr[497] were sampled using BPMC [41] during the second step of the protocol. As previously described, this resulted in the generation of 47 SERT binding pocket conformations [37], out of which the three, with the lowest energy were used for ensemble docking (Fig S1, supplementary materials).

Preliminary docking revealed (see results) that further modification of SERT models was necessary to dock such large compounds. Thus, two complexes with the lowest score, but with oppositely oriented ligands (**9** and **13**), were selected for refinements using induced fit (Fig S1, supplementary materials). During the refinement, the side chain torsion angles of the amino acids within 4.0 Å of the ligands were changed in each random step using the BPMC procedure [41].

All ligands, including quipazine and 6-nitroquipazine, were docked to the two different SERT conformations obtained after induced fit refinement by using usual rigid protein-flexible ligand approach (four parallel dockings performed).

2.4.4. Modelling of ligands

The examined ligands (Table 1) were protonated at the nitrogen atom attached to the butyl fragment. Ligands **12**, **14**, **15**, **16**, **18** of the quipazine analogues and **3**, **5**, **7** of the nitroquipazine analogues additionally possessed a methyl group in an alpha position with respect to the protonated nitrogen atom. Structures of the ligands were constructed based on the X-ray structure of buspirone [16] using the ICM program [39].

3. Results

3.1. Binding affinities

Our studies showed that 6-nitroquipazine buspirone analogues have lower affinity than the quipazine derivatives (Table 1).

Comparison of binding affinities of six pairs of methylated and non-methylated quipazine analogues (**12**−**13**, **16**−**17**, **18**−**19**) and nitro-quipazine analogues (**3**−**4**, **5**−**6** and **7**−**8**) showed that introduction of the methyl group gave relatively higher binding affinities and complex stabilization (for the four pairs: **4**→**3**, **6**→**5**, **13**→**12**, and **17**→**16**) or no change (or minor loss) of binding affinity and complex destabilization (for two of the pairs: **8**→**7**, **19**→**18**) for SERT (Table 1). Compound **14** with shorter n-propyl chain exhibited slightly lower affinity than the n-butyl analogue **12**.

Compound **11**, with an amide substituent at C6 position of the quinoline moiety, showed higher affinity for SERT than compound **6**. The 5-chloroquipazine analogue **10** showed lowest affinity of all derivatives possessing imide fragment (d) (**7**, **8**, **18**, **19**, Table 1).

3.2. SERT models

Three ligand binding pockets were identified in the SERT model representing the closed SERT conformation: the putative substrate binding pocket and two vestibular binding pockets that were fused into one before the docking (Fig. 5a). The putative substrate binding pocket consisted of amino acids within TMHs: 1, 3, 6 and 8, while amino acids in TMHs: 1, 3, 6, 10, 11 and EL4 constituted the fused vestibular binding pocket. Both binding regions were separated by a gate formed by Tyr[176] in TMH3 and Phe[335] in TMH6.

In the model representing the outward-facing SERT conformation the putative substrate binding pocket and the vestibular pocket created one larger binding pocket (Fig. 5b) that included amino acids from TMHs 1, 3, 6, 8, 10 and EL4.

3.3. Docking study

Docking of the compounds into the putative substrate binding site of the occluded SERT model indicated that the ligands were located in the pore formed between TMHs 1, 3, 6, 8 (Fig. 6a). However, only quipazine and nitroquipazine fitted well into the binding pocket and did not exhibit substantial unfavourable steric interactions (Fig. 7a−b, Fig S2-supplementary materials). Steric and electrostatic hindrance was observed between compounds **3**−**11** and amino acids forming the binding pocket. The nitroquipazine derivatives **3**−**9** had their NO$_2$ group located next to the charged amino acid Asp[400] that may cause electrostatic repulsion. The NO$_2$ group was also located close to Ile[179] and Trp[103] resulting in steric clashes with SERT. Steric interactions were also observed between the Cl substituent of the 5-chloroquipazine and Tyr[175] of SERT. The ligands **3**−**19** were close to Tyr[176] and Phe[335] and steric interactions were observed. Amino acids lining the putative binding pocket for quipazine and nitroquipazine were: Tyr[95], Ala[96], Asp[98], Gly[100] in
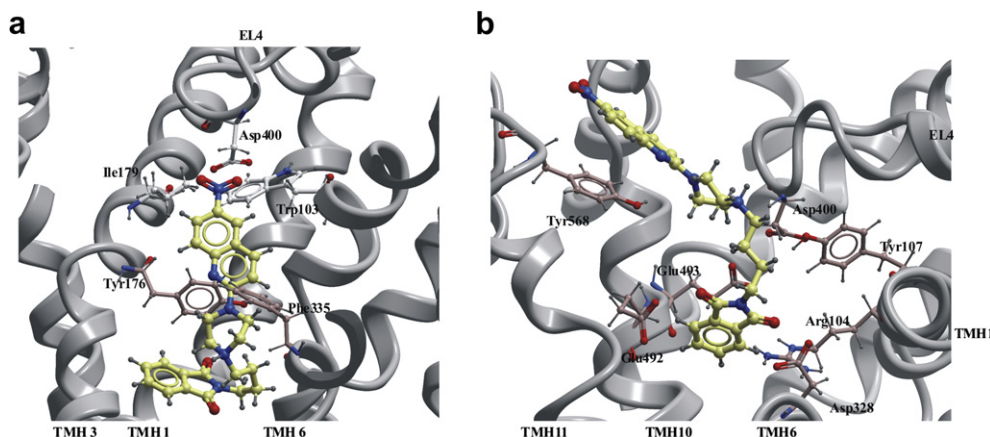

Fig. 6. The docking of nitroquipazine derivatives to the a) putative binding site, b) vestibular binding site of the SERT model in the closed conformation.
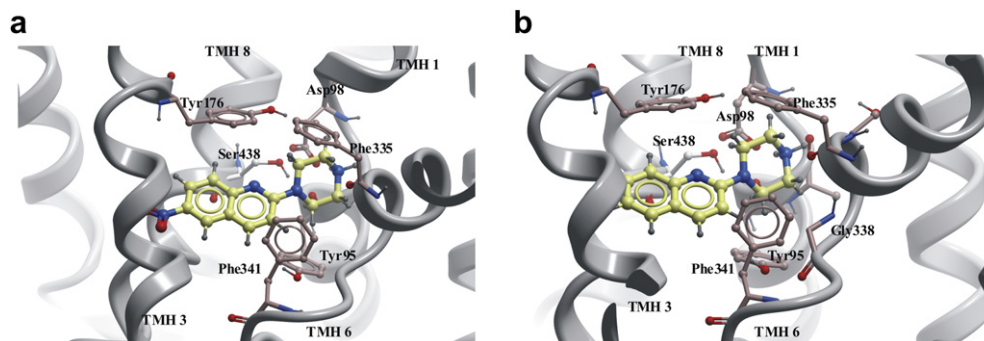
Fig. 7. The docking of a) 6-Nitroquipazine and b) quipazine to SERT model in closed conformation to the putative binding site. The amino acids Tyr[176] and Phe[355] form an aromatic lid that prevents from binding of long arylopiperazine analogues to SERT in closed conformation.

TMH 1; Ala[169], Phe[170], Ile[172], Ala[173], Tyr[176], Asn[177] in TMH 3; Phe[335], Ser[336], Leu[337], Gly[338], Phe[341] in TMH 6; Ser[438], Thr[439], Ala[441], Gly[442], Leu[443], Leu[444] in TMH 8.

Docking into the vestibular binding pocket, that corresponds to tricyclic antidepressant binding site in LeuT, showed that the compounds were too large for that binding site, and instead, they bound to the extracellular facing cavity surface region consisting of transmembrane helices: 1, 6, 10, 11 and extracellular loops EL4, EL5, EL6 (Fig. 6b, Fig S2-supplementary materials). The residues involved in the ligand binding to the surface regions were: Arg[104], Tyr[107], Gln[111] in TMH1; Ile[327], Asp[328], Ala[331] in TMH6; Lys[490], Glu[493], Glu[494] in TMH10, Phe[556] in TMH11 and Lys[399], Asp[400], Ala[401] in EL4, Tyr[487] in EL5, Arg[564], Tyr[568] in EL6. The ligands were located so their imide group was in close contact to charged amino acids: Asp[328], Glu[493], Glu[494].

The preliminary ligands docking to the outward-facing SERT model (three the lowest energy conformations, Fig S1- supplementary materials) showed that only quipazine, nitroquipazine, **9**, **13**, **14**, **16**, and **18** formed complexes with negative scores. Interestingly, quinoline moiety of **9** pointed toward EL4, whereas **13** was located with quinoline fragment directed to the bottom (intracellular side) of SERT model. Since other complexes were characterized by positive (unfavorable) scores and ligands **6** and **11** did not bind to any of the SERT conformations, a subsequent refinement step involving induced fit of complexes with **9** and **13** was performed. Re-docking into the two resulted SERT conformations showed that most of compounds followed binding mode of **9** (with the quinoline moiety next to EL4 and imide moiety at the bottom of the binding site; Fig S3- supplementary materials).

In that position the ligands were in contact with residues (Fig. 8a–b): Tyr[95], Ala[96], Asp[98], Gly[100], Asn[101], Trp[103], Arg[104], Tyr[107]

in TMH 1; Ile[172], Tyr[175], Tyr[176], Asn[177], Ile[179] in TMH 3; Phe[335], Ser[336], Leu[337], Gly[338], Phe[341] in TMH 6; Ser[438] in TMH 8, Glu[493], Thr[497] in TMH10 and Ala[399], Asp[400], Pro[403], Ser[404], Leu[405], Leu[406], Phe[407] in EL4. Only compound **5** was found to prefer a binding mode opposite to the others. All ligands adopted a folded conformations in the binding site. The methyl substituent in the piperazine ring was located equatorially in almost all the methylated compounds except for compounds **5, 7, 18** where the CH_3 group was in axial position. The substituent group of the buspirone analogues was placed next to the amino acids: Ala[399], Pro[403], Leu[405], Leu[406] in EL4 and Trp[103], Arg[104], Tyr[107] in TMH1.

4. Discussion

The function of SERT is to transport 5-HT from the synaptic cleft back into the presynaptic cell. Several studies indicate that widespread co-operative conformational changes including sliding and tilting motions of the TMHs may occur during ion and serotonin transport [45,46]. SERT may therefore involve several conformational changes during its transport cycle, both in TMHs and in loop segments, and it is not obvious which transporter conformation inhibitors prefer. Models representing different conformational states of SERT were therefore considered for docking in the present study (Fig. 5). The SERT model, constructed by homology to the LeuT crystal structures in complex with leucine, should correspond to a substrate-bound occluded conformation (Fig. 5a), while the model based on the X-ray structure of LeuT in complex with tryptophan should correspond to open-to-out conformation (Fig. 5b). The experimental data of ligand binding affinity (Table 1) together with molecular modelling studies provide the possibility of exploring the binding area of SERT.
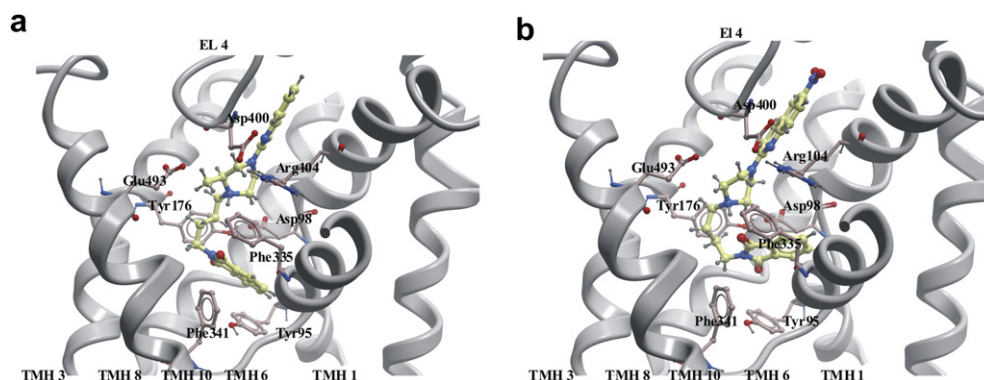

Fig. 8. The docking of nitrated and non-nitrated buspirone analogues to SERT model in outward-facing conformation: a) Ligand **12** b) Ligand **9**. The ligand were docked in similar manner with quinoline moiety located at the extracellular vestibule of SERT next to EL4 and imide moiety directed to the central cavity of SERT.

When constructing homology models of transporter proteins in general there are pitfalls in regard to several of the main steps in the homology modeling procedure. The accuracy of homology models depends on the sequence identity and functional similarity between the template and target proteins, the amino acid sequence alignments between the template and the targets and the resolution at which the template protein crystal structure was solved [47,48]. For membrane transporters in general there are few templates available, and the resolution of these templates is generally low. Furthermore, the homology between the target transporter and the template may also be low. Docking into homology based models of transporter proteins is therefore also challenging. In the present study the best docking results were obtained with open-to-out SERT model using the same docking protocol and open-to-out SERT model conformations as in our previous study [37]. In that study docking of a test set of actives and decoys indicated that the open-to-out model and the present docking protocol were able to score the majority of the active compounds above decoys.

Since the substitution at C6 position of the quinoline ring of compound **2** with a nitro group yields compound **1** with a much higher SERT affinity [25,26]. However, the NO_2 substituted buspirone derivatives show moderate SERT affinity, and lower than unsubstituted analogues. Further, a methyl group connected to the piperazine ring seems favourable, but not for compounds **7** and **18** (Table 1). The chloro- (**10**) and amide- (**11**) analogues posses lower affinity for SERT than did their counterparts without these groups (compounds **6**, **17** and **8**, **19**, respectively).

The experimental binding studies of the 6-nitroquipazine buspirone analogues **3**−**9** showed also the low binding affinity of these compounds toward 5-HT$_{1A}$ receptor (Table 1). The 5-HT$_{1A}$ receptor activity of the quipazine analogues was reported previously [16−19]. The affinity for other CNS targets has not been tested.

Docking to the closed conformation of SERT (Figs. 6 and 7) indicated that the binding pocket lacks space to accommodate the long-chain arylopiperazine derivatives, resulting in steric hindrance between the compounds and amino acids of the putative binding pocket (Fig. 7). Among the amino acids responsible for that were Tyr[176] in TMH3 and Phe[335] in TMH6 which together form an aromatic lid normally occluding the substrate binding site from the extracellular vestibule in SERT model in the closed conformation. The distance between Tyr[176] and Phe[335] is approximately 2.4 Å in the closed conformation, while in the open-to-out conformation the distance is 4.4 Å. Therefore, SERT in outward-facing conformation can accommodate in the binding site compounds with different size from smaller, such as quipazine, to larger, such as the buspirone analogues (Fig. 8). In addition, in the open-to-out conformation the distance between side chains of Arg[104] in TMH1 and Glu[493] in TMH10 is larger than in the model of SERT in the closed state, where these amino acids form a salt bridge. However, steric conflicts were observed for the buspirone analogues with nitro-, acetamide- or chloro- substituents located next to amino acids in TMH 1, 6 and EL4.

Ligand docking to the vestibular binding pocket of the closed SERT conformation indicated that the compounds were located in the region consisting of the extracellular loops: EL4, EL5, EL6. These loops are flexible, especially EL4 that is known to be important for the transport mechanism [58]. Thus, the docking of the ligands into the extracellular facing cavity of SERT indicated only weak interactions with the binding site. However, it cannot be ruled out that other compounds can bind to this pocket with substantial strength.

Our results showed that all nitrated and non-nitrated quipazine buspirone analogues were bound in the large binding pocket of the open-to-out SERT model. This pocket is formed by TMHs 1, 3, 6, 8, 10 and EL4 (Fig. 8a−b). Evidence from many laboratories confirm

involvement of amino acids in TMH1 [7,8,49,50], TMH3 [49,51−53], TMH6 [54,55] and TMH8 [56] for binding of compounds to SERT. Experimental accessibility studies of SERT indicate that also TMH10 might participate in the transition to a cytoplasmic-facing SERT conformation [57]. Mutagenesis studies involving amino acids in EL4 also indicated a role of this loop in the conformational changes associated with substrate transport [58].

Docking into the large binding pocket of the open-to-out SERT model indicated that the compounds preferred poses where the quinoline moiety was situated in the extracellular vestibule of SERT next to: Trp[103], Arg[104], Tyr[107] in TMH1 and Ala[398], Lys[399], Asp[400], Pro[403], Ser[404], Leu[405], Phe[407] in EL4 with the imide moiety deeper inside in the model close to: Ala[96], Tyr[95] in TMH1; Tyr[175], Tyr[176] in TMH3; Phe[341] in TMH6 and Thr[497] in TMH10 of SERT. Interactions between the nitrogen atom in the quinoline moiety and Arg[104] in TMH1 were observed. The C−H…π interactions between the C−H group of the amino acids Tyr[103] and Tyr[107] in TMH1 and quinoline moiety of the ligand might be important for binding of quipazine like buspirone analogues. The ligands in SERT were located near Phe[407] in EL4 that is the most conserved amino acid in all known sequences of the NSS family. The experimental data are suggesting that Phe[407] may play an important structural role [58]. The involvement of amino acids Tyr[103] in TMH1 and Ile[179] in TMH3 in a conformational change associated with SERT transport was also confirmed experimentally [64]. Hydrogen bonding interactions between the side chains of Tyr[95] in TMH1, Tyr[175] and Tyr[176] in TMH3, Ser[438] in TMH8 and imide group of the buspirone analogues
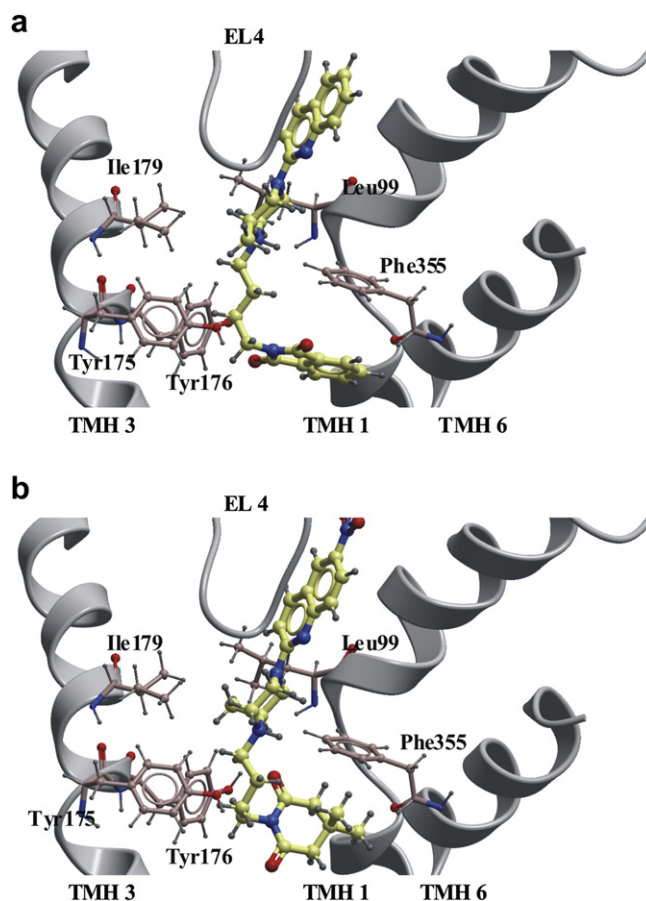

Fig. 9. The interactions between methyl group at the piperazine ring of buspirone analogues with SERT model in the outward-facing conformation: (a) Ligand **12** (b) Ligand **18**.

without substituent at the quinoline moiety seemed to stabilize the SERT-compound complexes.

Introduction of the nitro substituent to the quinoline led to rod-shaped compounds with two large polar groups at both ends. The nitrated buspirone analogues had the NO_2 group next to EL4. The presence of this polar group next to hydrophobic amino acids forming extracellular loop 4 can result in steric interactions between the compounds and SERT.

The amide substituted buspirone derivative **11** obtained low (positive) scoring values after docking to the SERT model in the open-to-out conformation which is in agreement with the experimental results (Table 1).

For compounds **3**, **12**, **14**, **15**, which possess a methyl group in the piperazine ring, weak C–H...π interactions between the hydrogen atoms of the methyl group and the aromatic moiety of Tyr[175] in TMH3 or Phe[335] (TMH 6) was observed (Fig. 9a). These weak interactions may play an important role during ligand-receptor complex formation and stabilization [59,60]. However, for compounds **7** and **18**, (as compared to **8** and **19**, respectively) an increase of binding affinity was not observed (Table 1). It should be noted that these compounds possess two additional methyl groups in their imide ring. For the complexes of SERT with ligands **7** and **18** the methyl group was directed toward hydrophobic amino acids: Ile[179] in TMH3 and Leu[99] in TMH1, and interactions between the methyl group and Phe[355] in TMH6 were not observed (Fig. 9b). In addition, the methyl group was located in the axial position in ligands: **5**, **7**, **18**, instead of the less hindered equatorial. It seems that Phe[355] in TMH 6 can play important roles in ligand binding to SERT.

5. Conclusions

In the present paper, synthesis, binding studies and docking of a series of buspirone analogues (**3**–**11**) that target the SERT have been described. We also performed docking of a series of compounds from a previous study (**12**–**19**). The introduction of a nitro, amide or chloro substituent into the buspirone analogues resulted in reduced SERT binding affinity. The compounds were docked to two different SERT models that should represent a closed conformation and an outward-facing (open-to-out) conformation of SERT. The docking indicated that the SERT model in open-to-out conformation could accommodate all studied compounds in the binding pocket, and seems to represent the most reliable model for binding these compounds. The docking also showed that the introduction of a nitro, amide or chloro substituent into the buspirone analogues resulted in steric clashes with amino acids of SERT that may explain their reduced affinities for SERT.

6. Experimental protocols

6.1. General procedure for the preparation of N-(4-bromobutyl) imides **25**–**28**

To the solution of an imide of general structure **B** in dry toluene anhydrous K_2CO_3 (2.5 equiv), 18-crown-6 (1 mol %) and 1,4-dibromobutane (4 equiv) were added. The reaction mixture was stirred under reflux for 24 h under inert gas. Then, the reaction mixture was filtered off and the filter cake washed with dichloromethane. The combined filtrates were evaporated under reduced pressure and crude product was distilled under reduced pressure.

6.1.1. 1-(4-Bromobutyl)-piperidine-2,6-dione (**25**)

From glutarimide (**21**) and 1,4-dibromobutane: bright yellow oil (89%). ^{1}H NMR (CDCl3) δ (ppm) = 3.78 (t, 2H, J = 7.1 Hz), 3.41 (t, 2H, J = 6.5 Hz), 2.65 (t, 4H, J = 6.55 Hz), 1.78–1.88 (m, 4H), 1.61–1.73 (m, 2H); ^{13}C NMR (CDCl3) δ (ppm) = 172.3, 38.37, 33.0, 32.7, 29.9, 26.6,

17.0. IR (CHCl3): v (cm^{-1}) = 1725, 1671; R_f = 0.28 (30% AcOEt/hex); b.p. = 197 °C/3 tor. Spectroscopic data consistent with reported previously [61].

6.1.2. 1-(4-bromobutyl)-4,4-dimethylpiperidine-2,6-dione (**26**)

From 3,3-dimethylglutarimide (**22**) and 1,4-dibromobutane: bright yellow oil (83%). ^{1}H NMR (CDCl3) δ (ppm) = 3.79 (t, 2H, J = 7.1 Hz), 3.41 (t, 2H, J = 6.5 Hz), 2.5 (s, 4H), 1.83–1.89 (m, 2H), 1.03–1.70 (m, 2H), 1.08 (s, 6H); ^{13}C NMR (CDCl3) δ (ppm) = 171.8, 46.3, 38.35, 32.9, 30.08, 29.0, 27.6, 26.6; IR (CHCl3): v (cm^{-1}) = 1724, 1671; R_f = 0.38 (30% AcOEt/hex); b.p. = 205 °C/3 tor. Spectroscopic data consistent with reported previously [61,62].

6.1.3. 8-(4-bromobutyl)-8-azaspiro[4.5]decane-7,9-dione (**27**)

From 3,3-tetramethyleneglutarimide (**23**) and 1,4-dibromobutane: bright yellow oil (75%). ^{1}H NMR (CDCl3) δ (ppm) = 3.79 (t, 2H, J = 7.1 Hz), 3.41 (t, 2H, J = 6.5 Hz), 2.59 (s, 4H), 1.81–1.85 (m, 2H), 1.65–1.78 (m, 6H), 1.47–1.53 (m, 4H); ^{13}C NMR (CDCl3) δ (ppm) = 171.9, 44.5, 39.2, 38.14, 37.27, 32.8, 29.8, 26.4, 23.9; IR (CHCl3): v (cm^{-1}) = 1724, 1668; R_f = 0.41 (30% AcOEt/hex), b.p. = 215 °C/3 tor. Spectroscopic data consistent with reported previously [61,62].

6.1.4. N-(4-bromobutyl)isoindoline-1,3-dione (**28**)

From phthalimide (**24**) and dibromobutane: white crystals (83%). ^{1}H NMR (CDCl3) δ (ppm) = 7.82–7.87 (m, 2H), 7.69–7.74 (m, 2H), 3.72 (t, 2H, J = 6.6 Hz), 3.44 (t, 2H, J = 6.3 Hz), 1.86–1.91 (m, 4H); ^{13}C NMR (CDCl3) δ (ppm) = 168.2, 133.9, 131.9, 123.1, 36.8, 32.7, 29.7, 27.1; IR (CHCl3): v (cm^{-1}) = 1618, 1604, 1507; R_f: 0.59 (30% AcOEt/hex), b.p. = 230 °C/3 Tor. Spectroscopic data consistent with reported previously [63].

6.2. General procedure of 6-nitroquipazine (**1**) and 3′-methyl-6-nitroquipazine (**20**) N-alkylation

To the solution of 6-nitroquipazine (**1**) or 3′-methyl-6-nitroquipazine (**20**) in dry toluene were added anhydrous K_2CO_3 (4 equiv.), 18-crown-6 (0.01 equiv.) and 1-(4-bromobutyl)imide of general structure **A** (Fig. 2, 2 equiv.) were added and the mixture was stirred under refluxed for 5 days. Then the reaction mixture was filtrated and the filter cake washed with dichloromethane (DCM). The combined filtrates were evaporated under reduced pressure. The crude product was purified by column chromatography on silica gel (0–3% MeOH in DCM).

6.2.1. 1-{4-[2-methyl-4-(6-nitro-quinolin-2-yl)piperazin-1-ylo] butyl}piperidine-2,6-dione (**3**)

From 3′-methyl-6-nitroquipazine (**20**) and 1-(4-bromobutyl) piperidine-2,6-dione (**25**). Brown solid. ^{1}H NMR (CDCl3) δ (ppm) = 8.49 (d, 1H, J = 2.54), 8.26 (dd, 1H, J_1 = 2.62, J_2 = 9.21), 7.92 (d, 1H, J = 9.29), 7.62 (d, 1H, J = 9.24), 7.03 (d, 1H, J = 9.37), 4.30–4.20 (m, 2H), 3.85–3.75 (m, 2H), 3.50–3.35 (m, 1H), 3.15–2.90 (m, 2H), 2.64 (t, 4H, J = 6.57), 2.45–2.25 (m, 4H), 2.00–1.90 (m, 2H), 2.60–2.40 (m, 4H), 1.13 (d, 3H, J = 6.18). ^{13}C NMR (CDCl3) δ (ppm) = 172.3, 158.1, 141.5, 138.4, 126.8, 124.0, 123.4, 120.8, 110.6, 54.6, 52.8, 51.0, 44.7, 39.2, 32.7, 25.9, 23.3, 17.0, 15.6; R_f = 0.35 (10% MeOH/DCM).

3•HCl; C23H29N5O4•HCl m.p. = 203 °C-206 °C. Anal. calcd. for $C_{23}H_{29}N_5O_4 \cdot HCl$ 0.33H2O: C, 57.32; H, 6.41; N, 14.53; Found: C, 57.34; H, 6.53; N, 14.27%.

6.2.2. 1-{4-[4-(6-Nitro-quinolin-2-yl)-piperazin-1-yl]-butyl}-piperidine-2,6-dione (**4**)

from 6-nitroquipazine (**1**) and 1-(4-bromobutyl)piperidine-2,6-dione (**25**). 60% dark brown semi-solid. ^{1}H NMR (CDCl3)

δ (ppm) = 8.52 (d, 1H, J = 2.6 Hz), 8.28 (dd, 1H, J_1 = 2.5 Hz, J_2 = 9.22 Hz), 7.95 (d, 1H, J = 9.27 Hz), 7.64 (d, 1H, J = 9.24 Hz), 7.05 (d, 1H, J = 9.29 Hz), 3.87–3.76 (m, 6H), 2.68–2.54 (m, 6H), 2.45–2.38 (m, 4H), 1.93 (t, 4H, J = 6.38), 1.61–1.53 (m, 2H). R_f: 0.45 (10% MeOH/DCM).

4•HCl: $C_{22}H_{27}N_5O_4$•HCl; m.p. = 180 °C-182 °C.

^{1}H NMR (CDCl$_3$) δ(ppm) = 8.78 (d,1H J = 2.57 Hz), 8.38 (d,1H, J = 9.3 Hz), 8.25 (dd, 1H, J_1 = 2.63 Hz, J_2 = 2.63 Hz), 7.67 (d, 1H, J = 9.25 Hz), 7.5 (d, 1H, J = 9.3 Hz), 4.78 (d, 2H, J = 5.24), 3.65–3.55 (m, 6H), 3.12–3.04 (m, 4H), 2.6 (t, 4H, J = 6.44), 1.89–1.64 (m, 4H), 1.58–1.43 (m, 2H);

Anal. calcd for $C_{22}H_{27}N_5O_4$•HCl•0.5H$_2$O: C, 56.11; H, 6.21; N, 14.87%. Found: C, 55.94; H, 6.17; N, 14.77%.

6.2.3. 8-{4-[2-methyl-4-(6-nitro-quinolin-2-yl)-piperazin-1-yl]-butyl}-8-azaspiro[4.5]-decane-7,9-dione (*5*)

From 3′-methyl-6-nitroquipazine (**20**) and 8-(4-bromobutyl)-8-azaspiro[4.5]decane-7,9-dione (**27**). Brown semi-solid 60%. ^{1}H NMR(CDCl$_3$) δ (ppm) = 8.52 (d, 1H, J = 2.56), 8.29 (dd, 1H, J_1 = 2.54, J_2 = 9.22), 7.95 (d, 1H, J = 9.33), 7.65 (d, 1H, J = 9.24), 7.05 (d, 1H, J = 9.35), 4.25 (d, 2H, J = 12.94), 3.79 (t, 2H, J = 6.62), 3.49–3.40 (m, 1H), 3.15–3.07 (m, 1H), 3.03–2.93 (m, 1H), 2.79–2.70 (m, 1H), 2.59 (s, 4H), 2.53–2.50 (m, 1H), 2.42–2.32 (m, 2H), 1.75–1.65 (m, 6H), 1.54–1.50 (m. 10H), 1.15 (d, 3H, J = 6.18); ^{13}C NMR (CDCl$_3$) δ (ppm) = 172.0, 158.1, 151.4, 141.7, 138.3, 126.8, 124.0, 123.3, 120.7, 110.6, 54.5, 52.8, 51.0, 50.2, 44.7, 39.3, 39.1, 37.3, 25.8, 24.0, 23.1, 15.6; R_f: 0.46 (10% MeOH/DCM).

5•HCl: $C_{27}H_{35}N_5O_4$•HCl; m.p. 192–195 °C. Anal. calcd for $C_{27}H_{35}N_5O_4$•HCl•0.5H$_2$O: C, 60.16; H, 6.92; N, 12.99%. Found: C, 60.15; H, 7.08; N, 12.99%.

6.2.4. 8-{4-[4-(6-Nitro-quinolin-2-yl)-piperazin-1-yl]-butyl}-8-azaspiro[4.5]decane-7,9-dione (*6*)

From 6-nitroquipazine (**1**) and 8-(4-bromobutyl)-8-azaspiro[4.5]decane-7,9-dione (**27**). Dark brown oil 67%.^{1}H NMR (CDCl$_3$) δ (ppm) = 8.53 (d, 1H, J = 2.5 Hz), 8.28 (dd, 1H, J_1 = 2.53 Hz, J_2 = 9.21 Hz), 7.95 (d, 1H, J = 9.31 Hz), 7.65 (d, 1H, J = 9.2 Hz), 7.05 (d, 1H, J = 9.4 Hz), 3.88–3.76 (m, 6H), 2.59–2.54 (m, 8H), 2.42 (t, 2H, J = 6.8), 1.75–1.68 (m, 4H), 1.63–1.47 (m, 6H); ^{13}C NMR (CDCl$_3$) δ (ppm) = 172.1, 158.3, 151.4, 141.6, 138.5, 126.9, 124.1, 123.4, 120.9, 110.7, 58.0, 52.9, 44.7, 44.5, 39.6, 39.2, 37.4, 29.9, 25.8, 24.1; R_f: 0.54 (10% MeOH/DCM).

6•HCl: $C_{26}H_{33}N_5O_4$•HCl, m.p. 193–194 °C.

^{1}H NMR (CDCl3) δ (ppm) = 8.81 (d, 1H, J = 2.46 Hz), 8.42 (d, 1H, J = 9.32 Hz), 8.31 (dd, 1H, $J1$ = 2.7 Hz, $J2$ = 2.78 Hz), 7.77 (d, 1H, J = 9.22 Hz), 7.54 (d, 1H, J = 9.33 Hz), 4.78 (d, 2H, J = 13.8), 3.69–3.55 (m, 6H), 3.09 (s, 4H), 2.62 (s, 4H), 1.8–1.65 (m, 2H), 1.62–1.59 (m, 4H), 1.48–1.41 (m, 6H);

Anal. calcd for $C_{26}H_{33}N_5O_4$•HCl•0.5H$_2$O: C, 59.48; H, 6.72; N, 13.34%. Found: C, 59.49; H, 6.93; N, 13.25%.

6.2.5. 4,4-Dimethyl-1-{4-[2-methyl-4-(6-nitro-quinolin-2-yl)-piperazin-1-yl]-butyl}-piperidine-2,6-dione (*7*)

From 3′-methyl-6-nitroquipazine (**20**) and 1-(4-bromobutyl)-4,4-dimethylpiperidine-2,6-dione (**26**). Brown semi oil 52%. ^{1}H NMR(CDCl$_3$) δ (ppm) = 8.51 (d, 1H, J = 2.59), 8.28 (dd, 1H, J_1 = 2.65, J_2 = 9.26), 7.94 (d, 1H, J = 9.30), 7.64 (d, 1H, J = 9.27), 7.05 (d, 1H, J = 9.34), 4.26 (d, 2H, J = 12.94), 3.80 (t, 2H, J = 6.70), 3.49–3.37 (m, 1H), 3.14–3.08 (m, 1H), 3.03–2.92 (m, 1H), 2.80–2.74 (m, 1H), 2.56–2.50 (m, 1H), 2.50 (s, 4H), 2.44–2.32 (m, 2H), 1.54–1.25 (m, 4H), 1.14 (d, 3H, J = 6.22), 1.08 (s, 6H); ^{13}C NMR (CDCl$_3$) δ (ppm) = 171.8, 158.2, 151.5, 141.6, 138.5, 126.9, 124.1, 123.5, 120.8, 110.7, 54.6, 52.9, 51.1, 50.3, 46.3, 44.7, 39.2, 29.0, 27.6, 25.9, 23.3, 15.6; R_f = 0.45 (10% MeOH/DCM).

7•HCl: $C_{25}H_{33}N_5O_4$•HCl; m.p. 177–181 °C.

Anal. Calcd for $C_{25}H_{33}N_5O_4$•HCl•0.5H$_2$O: C, 58.53; H, 6.88; N, 13.65%. Found: C, 58.36; H, 7.03; N, 13.66%.

6.2.6. 4,4-Dimethyl-1-{4-[4-(6-nitro-quinolin-2-yl)-piperazin-1-yl]-butyl}-piperidine-2,6-dione (*8*)

From 6-nitroquipazine (**1**) and 1-(4-bromobutyl)-4,4-dimethylpiperidine-2,6-dione (**26**): 60% dark brown oil. ^{1}H NMR (CDCl$_3$) δ (ppm) = 8.52 (d, 1H, J = 2.6 Hz), 8.28 (dd, 1H, J_1 = 2.6 Hz, J_2 = 9.25 Hz), 7.95 (d, 1H, J = 9.33 Hz), 7.65 (d, 1H, J = 9.24 Hz), 7.05 (d, 1H, J = 9.28 Hz), 3.88–3.76 (m, 6H), 2.57 (t, 6H, J = 4.9 Hz), 2.50 (s, 4H), 2.42 (t, 2H, J = 6.8 Hz), 1.56 (t, 4H, J = 3.55 Hz), 1.08 (s, 6H); ^{13}C NMR (CDCl$_3$) δ (ppm) = 171.8, 158.2, 151.3, 141.6, 138.4, 126.8, 124.0, 123.4, 120.8, 110.7, 57.9, 52.8, 46.2, 44.4, 38.9, 29.7, 28.9, 27.4, 25.7; R_f: 0.38 (10% MeOH/DCM).

8•HCl: $C_{24}H_{31}N_5O_4$•HCl, m.p. 173 °C-174 °C.

^{1}H NMR (CDCl$_3$) δ (ppm) = 8.79 (d, 1H, J = 2.65 Hz), 8.4 (d, 1H, J = 9.36 Hz), 8.29 (dd, 1H, J_1 = 2.6 Hz, J_2 = 2.71 Hz), 7.78 (d, 1H, J = 9.27 Hz), 7.51 (d, 1H, J = 9.4 Hz), 4.76 (d, 2H, J = 13.77), 3.7–3.5 (m, 7H), 3.1–3.05 (m, 4H), 2.54 (s, 4H), 1.85–1.7 (m, 2H), 1.49–1.45 (m, 2H), 0.98 (s, 6H).

Anal. calcd for $C_{24}H_{31}N_5O_4$•HCl•0.5H$_2$O: C, 57.77; H, 6.67; N, 14.03%. Found: C, 57.67; H, 6.74; N, 13.95%.

6.2.7. 2-{4-[4-(6-Nitro-quinolin-2-yl)-piperazin-1-yl]-butyl}-isoindole-1,3-dione (*9*)

From 6-nitroquipazine (**1**) and 2-(4-bromobutyl)-1H-isoindole-1,3(2H)-dione (**28**). Dark brown crystals 61%. ^{1}H NMR (CDCl$_3$) δ (ppm) = 8.52 (d, 1H, J = 2.55 Hz), 8.28 (dd, 1H, J_1 = 2.67 Hz, J_2 = 9.26 Hz), 7.95 (d, 1H, J = 9.32 Hz), 7.87–7.82 (m, 2H), 7.76–7.69 (m, 2H), 7.64 (d, 1H, J = 9.28), 7.05 (d, 1H, J = 9.35), 3.85 (t, 4H, J = 5.02), 3.73 (t, 2H, J = 6.89), 2.57 (t, 2H, J = 4.99), 2.45 (t, 2H, J = 7.25), 1.80–1.59 (m, 4H); R_f: 0.41 (10% MeOH/DCM).

9•HCl: $C_{25}H_{25}N_5O_4$•HCl; m.p. 219 °C-220 °C.

^{1}H NMR (CDCl$_3$) δ (ppm) = 8.77 (d, 1H, J = 2.66 Hz), 8.38 (d, 1H, J = 9.35 Hz), 8.27 (dd, 1H, J_1 = 2.59 Hz, J_2 = 2.72 Hz), 7.66 (d, 1H, J = 9.23 Hz), 7.49 (d, 1H, J = 9.3 Hz), 4.71 (d, 2H, J = 13.8 Hz), 3.64–3.57 (m, 6H), 3.27–3.12 (m, 4H), 1.77–1.65 (m, 4H).

Anal. calcd for $C_{25}H_{25}N_5O_4$•HCl•0.5H$_2$O: C, 59.46; H, 5.39; N, 13.87%. Found: C, 60.26; H, 5.49; N, 13.85%.

6.3. Preparation of compounds *10* and *11*

6.3.1. 1-{4-[4-(5-chloroquinolin-2-yl)piperazin-1-yl]butyl}-4,4-dimethylopiperydine-2,6-dione (*10*)

To the solution of 5-chloroquipazine (**29**) (1.223 g, 4.9 mmol) in 40 mL of anhydrous toluene 2.74 g, (2 equiv.) of bromoimide (**26**), 2.76 g (4 equiv.) of anhydrous potassium carbonate and 0.19 g of 18-crown-6 were added. The reactions mixture was heated under reflux for 4 days. The resulted suspension was filtered off and the residue was evaporated. Combined solid residues were purified with the aid of column chromatography on silica gel (0–3% MeOH/DCM) to give brown oil of **10** (0.940, 43%). ^{1}H NMR (CDCl$_3$) δ (ppm) = 8.22 (d, 1H, J = 9.36 Hz), 7.56 (d, 1H, J = 7.62 Hz), 7.63 (d, 1H, J = 8.95 Hz), 7.38 (t, 1H, J = 8.41 Hz), 7.38 (dd, 1H, J_1 = 7.60 Hz, J_2 = 8.40 Hz), 6.98 (d, 1H, J = 9.40 Hz), 3.77 (t, 2H, J = 6.76 Hz), 3.73 (t, 4H, J = 4.88 Hz), 2.52 (t, 4H, J = 5.00 Hz), 2.46 (s, 4H), 1.55–1.52 (m, 4H), 1.04 (s, 6H). ^{13}C NMR (CDCl$_3$) δ (ppm) = 171.7, 157.3, 148.7, 133.9, 130.9, 129.1, 125.6, 122.1, 120.7, 110.0, 77.0, 58.1, 52.9, 46.3, 44.8, 39.2, 29.0, 27.5, 25.9, 24.2; R_f = 0.25 (5% MeOH/DCM).

10•HCl: $C_{22}H_{33}N_5O_2$•HCl.

Anal. calcd. for $C_{22}H_{33}N_5O_2$•HCl•3H$_2$O: C, 55.92; H, 7.04; N, 10.87%. Found: C, 55.92; H, 6.85; N, 10.96%.

6.3.2. 8-{4-[4-(6-aminoquinolin-2-yl)piperazin-1-yl]butyl}-8-azaspiro-[4.5]decane-7,9-dione (*30*)

1-{4-[4-(6-Nitrochinolin-2-ylo)-piperazyn-1-ylo]butylo}-8-azaspiro[4.5]decano-7,9-dion (**6**) (0.325 g, 0.7 mmol) was dissolved in concentrated hydrochloric acid (8 mL) and 0.52 g (4 equiv.) of tin

(II) chloride was added. The reaction mixture was heated at 60 °C for 3 h, poured out on crushed ice, alkalized to pH 12 with 12 M NaOH do pH = 12 and extracted with DCM (3 × 50 mL). Combined organic layers were dried over anhydrous $MgSO_4$ and evaporated under reduced pressure. The residue was purified by column chromatography on silica gel (0–6% MeOH/DCM) to give 0.18 g (58%) of brown solid which was directly used to the next reaction. ^{1}H NMR (CDCl$_3$) δ (ppm) = 7.71 (d, 1H, J = 9.11 Hz), 7.57 (d, 1H, J = 8.85 Hz), 7.03 (dd, 1H, J_1 = 2.60 Hz, J_2 = 8.79 Hz), 6.92 (d, 1H. J = 9.13 Hz), 6.82 (d, 1H, J = 2.54 Hz), 3.79 (t, 2H, J = 6.69 Hz) 3.68 (t, 4H, J = 4.66 Hz), 2.62–2.56 (m, 8H), 2.45–2.40 (m, 2H), 1.75–1.67 (m, 4H), 1.59–1.47 (m, 8H). **IR** (CHCl$_3$): ν (cm^{-1}) = 3446,3374, 29571724, 1668, 1606, 1507; R_f = 0.42 (10% MeOH/DCM).

6.3.3. N-(2-{4-[4-(7,9-dioxo-8-azaspiro[4.5]dec-8-yl)butyl]piperazin-1-yl}quinolin-6-yl)-acetamide (11)

To the solution of compound **30** (0.17 g, 0.4 mmol) in glacial acetic acid (5 mL), acetic anhydride (0.36 mL, 10 equiv.) was added and the mixture was stirred at room temperature for 1 h. The reaction mixture was poured onto ice, alkalised with 12 M NaOH to pH = 12 and extracted with DCM (3 × 50 mL). The combined organic layers were dried over anhydrous $MgSO_4$ i evaporated to dryness. The resulted crude product was purified by column chromatography (0–6% MeOH/DCM) to give white-grey solid residue (0.193 g, 93%). ^{1}H NMR (CDCl$_3$) δ (ppm) = 8.06 (d, 1H, J = 2.23 Hz), 7.84 (d, 1H, J = 9.19 Hz), 7.63 (d, 1H, J = 8.95 Hz), 7.49 (s, 1H), 7.38 (dd, 1H, J_1 = 2.36 Hz, J_2 = 8.85 Hz), 6.96 (d, 1H, J = 9.18 Hz), 3.79–3.70 (m, 6H), 2.59–2.54 (m, 8H), 2.42–2.40(m, 2H), 2.20 (s, 3H), 1.75–1.67 (m, 4H), 1.54–1.50 (m, 8H). ^{13}C NMR (CDCl$_3$) δ (ppm) = 129.4, 128.0, 127.8, 127.5, 127.3, 127.1, 125.9, 56.1, 51.2, 48.7, 46.4, 20.0. IR (CHCl$_3$): ν (cm^{-1}) = 3437, 2956, 1724, 1668, 1609, 1533; R_f = 0.35 (10% MeOH/DCM).

11•HCl: $C_{22}H_{33}N_5O_2$•HCl.

Anal. calcd for $C_{22}H_{33}N_5O_2$•3 HCl•2.5H$_2$O: C, 52.06; H, 7.02; N, 10.84%. Found: C, 52.07; H, 7.20; N, 10.67%.

Acknowledgements

Appendix. Supplementary Data

Supplementary data related to this article can be found online at doi:10.1016/j.ejmech.2012.01.012.

References

[1] B.I. Kanner, E. Zomot, Sodium-coupled neurotransmitter transporters, Chem. Rev. 108 (2008) 1654–1668.
[2] P. Schlosss, D.C. Williams, The serotonin transporter: a primary target for antidepressant drugs, J. Psychopharmacol. 12 (1998) 115–121.
[3] J. Masson, C. Sagne, H. Hamon, S. El Mestikawy, Neurotransmitter transporters in the central nervous system, Pharmacol. Rev. 51 (1999) 439–464.
[4] J. Reizer, A. Reizer, H.H. Saier Jr., A functional superfamily of sodium/solute symporters, Biochim. Biophys. Acta 1197 (1994) 133–166.
[5] S. Ramamoorthy, A.L. Bauman, K.R. Moore, H. Han, T. Yang-Feng, A.S. Chang, Y. Gomapathy, R.D. Blakely, Antidepressant- and cocaine-sensitive human serotonin transporter: molecular cloning, expression, and chromosomal localization, Proc. Natl. Acad. Sci. USA 90 (1993) 2542–2546.
[6] S. Kitayama, T. Dohi, Cellular and molecular aspects of monoamine neurotransmitter transporters, J. Pharmacol. 72 (1996) 195–208.
[7] E.L. Barker, K.R. Moore, F. Rakhshan, R.D. Blakely, Transmembrane domain I contributes to the permeation pathway for serotonin and ions in the serotonin transporter, J. Neurosci. 19 (1999) 4705–4717.
[8] E.L. Barker, M.A. Perlman, E.M. Adkins, W.J. Houlihan, Z.B. Pristupa, H.B. Niznik, R.D. Blakely, High affinity recognition of serotonin transporter antagonists defined, by species-scanning mutagenesis. An aromatic residue in transmembrane domain I dictates, species-selective recognition of citalopram and mazindol, J. Biol. Chem. 273 (1998) 19459–19468.
[9] L. Iversen, Neurotransmitter transporters: fruitful targets for CNS drug discovery, Mol. Psychiatry 5 (2000) 357–362.
[10] S.M. Stahl, Mechanism of action of serotonin selective reuptake inhibitors: serotonin receptors and pathways mediate therapeutic effects and side effects, J. Aff. Dis. 5 (1998) 215–235.
[11] J.R. Homberg, D. Schubert, P. Gaspar, New perspectives on the neuro-developmental effects of SSRIs, Trends Pharmacol. Sci. 31 (2010) 60–65.
[12] P. Blier, C. de Montigny, Current advances and trends in treatment of depression, Trends Pharmacol. Sci. 15 (1994) 220–226.
[13] B.J. Jones, T.P. Blackburn, The medical benefit of 5-HT research, Pharmacol. Biochem. Behav. 71 (2002) 555–568.
[14] D.R. Thomas, D.R. Nelson, A.M. Johnson, Biochemical effects of the antidepressant paroxetine, a specific 5-hydroxytryptamine uptake inhibitor, Psychopharmacology 93 (1987) 193–200.
[15] D.T. Wong, K.W. Perry, F.P. Bymaster, The discovery of fluoxetine hydrochloride (Prozac), Nat. Rev. Drug Discov. 4 (2005) 764–774.
[16] Z. Chilmonczyk, A. Leś, A. Woźniakowska, J. Cybulski, A.E. Kozioł, M. Gdaniec, Buspirone analogues as ligands of the 5-HT1A receptor. 1. The molecular structure of buspirone and its two analogues, J. Med. Chem. 38 (1995) 1701–1710.
[17] K.J. Krajewski, A. Leś, J. Cybulski, Z. Chilmonczyk, A. Bronowska, A. Szelejewska-Woźniakowska, Novel buspirone-like 5-HT1A receptor ligands, Pol. J. Chem. 75 (2001) 71–78.
[18] Z. Chilmonczyk, M. Cybulski, J. Iskra-Jopa, E. Chojnacka-Wójcik, E. Tatarczyńska, A. Kłodzińska, A. Leś, A. Bronowska, I. Sylte, Interaction of 1,2,4-substituted piperazines, new serotonin receptor ligands, with 5-HT1A and 5-HT2A receptors, Il Farmaco 57 (2002) 285–301.
[19] J.K. Krajewski, Structure-activity relationship in a series of new 1,4-disubstituted piperazines as potential anxiolytic drugs. PhD thesis (polish), Warsaw 2001.
[20] M. Jarończyk, Z. Chilmonczyk, A.P. Mazurek, G. Nowak, A.W. Ravna, K. Kristiansen, I. Sylte, The molecular interactions of buspirone analogues with the serotonin transporter, Bioorg. Med. Chem. 16 (2008) 9283–9294.
[21] K. Hashimoto, T. Goromaru, High affinity binding of [^{3}H]6-nitroquipazine to cortical membranes in the rat: inhibition by 5-hydroxytryptamine and 5-hydroxytryptamine uptake inhibitors, Neuropharmacology 30 (1991) 113–117.
[22] K. Hashimoto, T. Goromaru, High-affinity binding of ['H]6- nitroquipazine to 5-hydroxytryptamine transporter in human platelets, Eur. J. Pharmacol. 187 (1990) 295–302.
[23] K. Hashimoto, T. Goromaru, Reduction of [3H]6-nitroquipazine-labelled 5-hydroxytryptamine uptake sites in rat brain by 3,4-methylenedio-xymethamphetamine, Fundam. Clin. Pharmacol. 4 (6) (1990) 635–641.
[24] K. Hashimoto, T. Goromaru, In vivo labeling of 5-hydroxytryptamine uptake sites in mouse brain with [3H]6-nitroquipazine, Pharmacol. Exper. Ther. 255 (1990) 146–153.
[25] A. Cappelli, G. Giuliani, A. Gallelli, S. Valenti, M. Anzini, L. Mennuni, F. Makovec, A. Cupello, S. Vomero, Structure-affinity relationship studies on arylpiperazine derivatives related to quipazine as serotonin transporter ligands. Molecular basis of the selectivity SERT/5HT3 receptor, Bioorg. Med. Chem. Lett. 13 (2005) 3455–3460.
[26] B.S. Lee, S. Chu, B.C. Lee, D.Y. Chi, Y.S. Choe, K.J. Jeong, C. Jin, Syntheses and binding affinities of 6-nitroquipazine analogues for serotonin transporter, Part 1. Bioorg. Med. Chem. Lett. 10 (2000) 1559–1562.
[27] J.M. Gerdes, S.C. DeFina, P.A. Wilson, S.E. Taylor, Serotonin transporter inhibitors: synthesis and binding potency of 2'-methyl- and 3'-methyl-6nitroquipazine, Bioorg. Med. Chem. Lett. 10 (2000) 2643–2646.
[28] B.S. Lee, S. Chu, B.-S. Lee, D.Y. Chi, Y.S. Song, C. Jin, Syntheses and binding affinities of 6-nitroquipazine analogues for serotonin transporter. Part 2: 4-substituted 6-nitroquipazines, Bioorg. Med. Chem. Lett. 12 (2002) 811–815.
[29] B.S. Moon, B.S. Lee, D.Y. Chi, Syntheses and binding affinities of 6-nitroquipazine analogues for serotonin transporter. Part 2: 3-alkyl-4-halo-6-nitroquipazines, Bioorg. Med. Chem. 13 (2005) 4952–4959.
[30] D. Zhou, G.P. Stack, J. Lo, A.A. Failli, D.A. Evrard, B.L. Harrison, N.T. Hatzenbuhler, M. Tran, S. Croce, S. Yi, J. Golembieski, G.A. Hornby, M. Lai, Q. Lin, L.E. Schechter, D.L. Smith, A.D. Shilling, C. Huselton, P. Mitchell, C.E. Beyer, T.H. Andree, Synthesis, Potency, and in vivo evaluation of 2-Piperazin-1-ylquinoline analogues as dual serotonin reuptake inhibitors and serotonin 5-HT1A receptor antagonists, J. Med. Chem. 52 (2009) 4955–4959.
[31] R. Perrone, F. Berardi, N.A. Colabufo, E. Lacivita, C. Larizza, M. Leopoldo, V. Tortorella, Design and synthesis of long-chain arylpiperazines with mixed affinity for serotonin transporter (SERT) and 5-HT1A receptor, JPP 57 (2005) 1319–1327.
[32] A. Yamashita, S.K. Singh, T. Kawate, Y. Jin, E. Gouaux, Crystal structure of a bacterial homologue of Na+/Cl- dependent neurotransmitter transporters, Nature 437 (2005) 215–223.
[33] M. Gabrielsen, A.W. Ravna, K. Kristiansen, I. Sylte, Substrate binding and translocation of the serotonin transporter studied by docking and molecular dynamics simulations, J. Mol. Model. (2011).doi:10.1007/s00894-011-1133-1.
[34] S.K. Satinder, C.L. Pisticelli, A. Yamashita, E. Gouaux, A comprehensive inhibitor traps LeuT in an open-to-out conformation, Science 322 (2008) 1655–1660.
[35] M.J. Owens, W.N. Morgan, S.J. Plott, C.B. Nemeroff, Neurotransmitter receptor and transporter binding profile of antidepressants and their metabolites, J. Pharmacol. Exp. Ther. 283 (1997) 1305–1322.

[36] D.N. Middlemiss, J.R. Fozard, 8-Hydroxy-2-(di-n-propylamino)-tetralin discriminates between subtypes of the 5-HT$_1$ recognition site, Eur. J. Pharmacol. 90 (1983) 151–153.

[37] M. Gabrielsen, R. Kurczab, A.W. Ravna, I. Kufareva, R. Abagyan, Z. Chilmonczyk, A.J. Bojarski, I. Sylte, Molecular mechanism of serotonin transporter inhibition elucidated by a new flexible docking protocol, Eur. J. Med. Chem. 47 (2012) 24–37.

[38] R. Apweiler, A. Bairoch, C.H. Wu, W.C. Barker, B. Boeckmann, S. Ferro, E. Gasteiger, H. Huang, R. Lopez, M. Magrane, M.J. Martin, D.A. Natale, C. O'Donovan, N. Redaschi, L.S. Yeh, UniProt: the Universal protein knowledgebase, Nucleic Acids Res. 32 (2004) 115–119.

[39] R. Abagyan, M. Totrov, D.N. Kuznetsow, ICM: a new method for protein modeling and design: applications to docking and structure prediction from the distorted native conformation, J. Comp. Chem. 15 (1994) 488–506.

[40] T. Beuming, L. Shi, J.A. Javitch, H. Weinstein, A comprehensive structure-based alignment of prokaryotic and eukaryotic neurotransmitter/ Na+ symporters (NSS) aids in the use of the LeuT structure to probe NSS structure and function, Mol. Pharmacol. 70 (2006) 1630–1642.

[41] R. Abagyan, M. Totrov, Biased probability Monte Carlo conformational searches and electrostatic calculations for peptides and proteins, J. Mol. Biol. 235 (1994) 983–1002.

[42] G. Bottegoni, I. Kufareva, M. Totrov, R. Abagyan, Four-dimensional docking: a fast and accurate account of discrete receptor flexibility in ligand docking, J. Med. Chem. 52 (2009) 397–406.

[43] M. Totrov, R. Abagyan, Flexible protein-ligand docking by global energy optimization in internal coordinates, Proteins(1) (1997) 215–220.

[44] M. Schapira, M. Totrov, R. Abagyan, Prediction of the binding energy for small molecules, peptides and proteins, J. Mol. Recog 12 (1999) 177–190.

[45] L.R. Forrest, G. Rudnick, The Rocking bundle: a mechanism for ion-coupled solute flux by symmetrical transporters, Physiology 24 (2009) 377–386.

[46] D.P. Claxton, M. Quick, L. Shi, F.D. de Carvalho, H. Weinstein, J. Javitch, H.S. Mchaourab, Ion/substrate-dependent conformational dynamics of a bacterial homolog of neurotransmitter: sodium symporters, Nat. Struct. Mol. Biol. 7 (2010) 822–830.

[47] C. Chothia, A.M. Lesk, The relation between the divergence of sequence and structure in proteins, Embo J. 5 (4) (1986) 823–826.

[48] L.R. Forrest, C.L. Tang, B. Honig, On the accuracy of homology modeling and sequence alignment methods applied to membrane proteins, Biophys. J. 91 (2) (2006) 508–517.

[49] L.K. Henry, J.R. Field, E.M. Adkins, M.L. Parnas, R.A. Vaughan, M. Zou, A.H. Newman, R.D. Blakely, Tyr-95 and Ile-172 in transmembrane segments 1 and 3 of human serotonin transporters interact to establish high affinity recognition of antidepressants, J. Biol. Chem. 281 (2006) 2012–2023.

[50] L.K. Henry, E.M. Adkins, O. Han, R.D. Blakely, Serotonin and cocaine-sensitive inactivation of human serotonin transporters by methanethiosulfonates targeted to transmembrane domain I, J. Biol. Chem. 278 (2003) 37052–37063.

[51] Z. Lin, W. Wang, T. Kopajtic, R.S. Revay, G.R. Uhl, Dopamine transporter: transmembrane phenylalanine mutations can selectively influence dopamine uptake and cocaine analog recognition, Mol. Pharmacol. 56 (1999) 434–447.

[52] O.V. Mortensen, A.S. Kristensen, O. Wiborg, Species-scanning mutagenesis of the serotonin transporter reveals residues essential in selective, high-affinity recognition of antidepressants, J. Neurochem. 79 (2001) 237–247.

[53] J.-G. Chen, A. Sachpatzidis, G. Rudnick, The third transmembrane domain of the serotonin transporter contains residues associated with substrate and cocaine binding, J. Biol. Chem. 272 (1997) 28321–28327.

[54] C. Roubert, P.J. Cox, M. Bruss, M. Hamon, H. Bonisch, B. Giros, Determination of residues in the norepinephrine transporter that are critical for tricyclic antidepressant affinity, J. Biol. Chem. 276 (2001) 8254–8260.

[55] Z. Lin, W. Wang, G.R. Uhl, Dopamine transporter tryptophan mutants highlight candidate dopamine- and cocaine-selective domains, Mol. Pharmacol. 58 (2000) 1581–1592.

[56] J. Andersen, O. Taboureau, K.B. Hansen, L. Olsen, J. Egebjerg, K. Strømgaard, A.S. Kristensen, Location of the antidepressant binding site in the serotonin transporter: importance of Ser-438 in recognition of citalopram and tricyclic antidepressants, J. Biol. Chem. 284 (2009) 10276–10284.

[57] Y.W. Zhang, G. Rudnick, The cytoplasmic substrate permeation pathway of serotonin transporter, J. Biol. Chem. 281 (2006) 36213–36220.

[58] S.M. Mitchell, E. Lee, M.L. Garcia, M.M. Stephan, Structure and function of extracellular loop 4 of the serotonin transporter as revealed by cysteine-scanning mutagenesis, J. Biol. Chem. 279 (2004) 24089–24099.

[59] M.J. Plevin, D.L. Bryce, J. Boisbouvier, Direct detection of CH/π interactions in proteins, Nat. Chem. 2 (2010) 466–471.

[60] M. Nishio, M. Hirota, Y. Umezawa, The CH/π Interaction. Evidence, Nature and Consequences, Wiley-VCH, New York, 1998.

[61] J.S. New, W.L. Christopher, J.P. Yevich, R. Butler Jr., R.F. Schlemmer, C.P. VanderMaelen, J.A. Cipollina, The thieno[3,2-c]pyridine and furo[3,2-c] pyridine rings: new pharmacophores with potential antipsychotic activity, J. Med. Chem. 32 (1989) 1147–1156.

[62] T. Podona, B. Guardiola-Lemaitre, D.H. Caignard, G. Adam, B. Pfeiffer, P. Renard, G. Guillaumet, 3,4-Dihydro-3-amino-2H-1-benzopyran derivatives as 5-HT1A receptor ligands and potential anxiolytic agents. 1. Synthesis and structure-activity relationship studies, J. Med. Chem. 37 (1994) 1779–1793.

[63] D.R. Hou, H.Y. Cheng, E.C. Wang, Efficient synthesis of oncinotine and neo-oncinotine, J. Org. Chem. 69 (2004) 6094–6099.

[64] Z. Thao, Y.-W. Zhang, A. Agyiri, G. Rudnick, Ligand effects on cross-linking support a conformational mechanism for serotonin transport, J. Biol. Chem. 284 (2009) 33807–33814.

[65] J. An, M. Totrov, R. Abagyan, Pocketome via comprehensive identification and classification of ligand binding envelopes, Mol. Cell Proteomics 4 (2005) 752–761.